Materials Research Express

ACCEPTED MANUSCRIPT • OPEN ACCESS

Nucleation and growth of discontinuous precipitates in Cu-Ag alloys

To cite this article before publication: Bailing An *et al* 2022 *Mater. Res. Express* in press https://doi.org/10.1088/2053-1591/ac5775

Manuscript version: Accepted Manuscript

Accepted Manuscript is "the version of the article accepted for publication including all changes made as a result of the peer review process, and which may also include the addition to the article by IOP Publishing of a header, an article ID, a cover sheet and/or an 'Accepted Manuscript' watermark, but excluding any other editing, typesetting or other changes made by IOP Publishing and/or its licensors"

This Accepted Manuscript is **© 2022 The Author(s). Published by IOP Publishing Ltd**.

As the Version of Record of this article is going to be / has been published on a gold open access basis under a CC BY 3.0 licence, this Accepted Manuscript is available for reuse under a CC BY 3.0 licence immediately.

Everyone is permitted to use all or part of the original content in this article, provided that they adhere to all the terms of the licence https://creativecommons.org/licences/by/3.0

Although reasonable endeavours have been taken to obtain all necessary permissions from third parties to include their copyrighted content within this article, their full citation and copyright line may not be present in this Accepted Manuscript version. Before using any content from this article, please refer to the Version of Record on IOPscience once published for full citation and copyright details, as permissions may be required. All third party content is fully copyright protected and is not published on a gold open access basis under a CC BY licence, unless that is specifically stated in the figure caption in the Version of Record.

View the article online for updates and enhancements.

This content was downloaded from IP address 146.201.201.48 on 01/03/2022 at 18:14

Nucleation and growth of discontinuous precipitates in Cu-Ag alloys

Bailing An[1, 2, 4], Yan Xin[4], Rongmei Niu[4], Zhaolong Xiang[1, 2, 4], Engang Wang[1, 3 *] and Ke Han[4 *]

[1] Key Laboratory of Electromagnetic Processing of Materials (Ministry of Education), Northeastern University, Shenyang, Liaoning, 110819, China

[2] School of Materials Science and Engineering, Northeastern University, Shenyang, Liaoning, 110819, China

[3] School of Metallurgy, Northeastern University, Shenyang, Liaoning, 110819, China

[4] National High Magnetic Field Laboratory, Florida State University, Tallahassee, 32310, FL, USA

[*] Corresponding authors

Engang Wang: Tel.: +86 24 836 81739, E-mail address: egwang@mail.neu.edu.cn

Ke Han: Tel.: +1 850 644 6746, E-mail address: han@magnet.fsu.edu

Abstract

To study discontinuous precipitation, which is an important method for strengthening materials, we observed the nucleation and growth of discontinuous precipitates in Cu-Ag alloys using electron backscatter diffraction and scanning transmission electron microscopy. We found that discontinuous precipitation always started with Ag precipitates, which nucleated on Cu grain boundaries. These precipitates then each took the shape of a large, abutted cone that shared a semi-coherent interface with one of the Cu grains, topped by a small spherical cap that shared an incoherent interface with the Cu grain on the opposite side of the boundary. This formation created a difference between the levels of interface energy on each side of boundary. We assume that this difference and boundary curvature together generates the driving force necessary to push grain boundary migration, thus triggering discontinuous precipitation. Because of grain boundary migration, Ag solute was consumed at one side of the grain, which causes a solute difference. The difference produces mainly driving force, pushing the boundaries to migrate forward.

Keywords: Cu-Ag alloys, discontinuous precipitation, nucleation and growth, grain boundary

Accepted Manuscript

migration

1. Introduction

Deformed Cu-24 wt%Ag alloys are widely used in high-field magnets as conductors because of their high strength and high conductivity [1-5]. The high strength is attributed to a high density of Ag fibers, which evolve from small-sized precipitates in as-cast alloys [1, 6-8]. Because of the cost of Ag, many researchers have reduced the Ag content to less than 8 wt%. In such alloys, discontinuous precipitates (DPs) usually occur [3, 9, 10].

Discontinuous precipitation has been observed in steels, Mg alloys, Ni alloys, and Cu alloys [11-17]. It is a solid-state reaction that usually has a migrating reaction front, which provides a conduit for fast solute transportation [18]. On both sides of the reaction front, crystal orientations and solute content are different [18, 19]. There are two nucleation mechanisms. The first one was proposed by Tu and Turnbull et al. who studied the DPs in Pb-Sn alloys [20, 21]. They assumed that the precipitates that lay on a habit plane and had an orientation relationship with the matrix had the minimum interfacial energy. Then, if the precipitates at grain boundaries lay on a habit plane on one side of grain, they cannot lie on the habit plane on the opposite side because of a tilt angle. This caused the different interfacial energy of the two sides, which formed a driving force to migrate the grain boundaries to remove the high-energy interface. The second one was proposed by Fournelle and Clark who studied discontinuous precipitation in Cu-In alloys [22]. They found that there was no definite habit plane and orientation relationship between In precipitates and Cu matrix. The driving force of initial grain boundaries migration may come from curved boundaries.

As far as we know, the nucleation of discontinuous precipitation needs further studies. Some researchers have tried to develop a unified principle to predict the nucleation of DPs from

Accepted Manuscript

two aspects, i.e., the lattice misfit between precipitates and matrix, and the difference between the atomic radius of solute and matrix, but neither is suitable [18, 23]. The nucleation sites of DPs are also under debate. Many studies have shown that high-angle grain boundaries are nucleation sites, but some studies showed that low-angle grain boundaries also nucleated DPs [18, 24, 25]. Monzen et al. stated that the high-energy grain boundaries were conducive to DPs nucleation and growth because they had high diffusivity [23, 26, 27].

In Cu-Ag alloys, many studies have focused on the growth rate and morphology of discontinuous precipitation during steady progress, but there is a lack of research on nucleation itself on an atomic scale [28-31]. Therefore, in this paper, we studied the nucleation and growth of DPs in Cu-6 wt%Ag and Cu-6wt%Ag-0.05 wt%Sc using Transmission Electron Microscopy (TEM), atomic resolution Scanning TEM (STEM), and Electron Backscatter Diffraction (EBSD).

2. Materials and methods

We cast Cu-6 wt%Ag and Cu-6wt%Ag-0.05 wt%Sc ingots in an induction furnace at a reduced pressure of 10^{-2} MPa. All the ingots were subjected to solution treatment in two steps: 760 °C for 4 h, and 790 °C for 6 h, then quenched in water. Afterwards, we cut several samples from each ingot and aged them at 450 °C for 15 min, 30 min, and 2 h in an argon atmosphere. Most of our data in this paper were from Cu-6 wt%Ag. To generate our findings with different chemistry, we also doped Sc. The role of doped Sc is shown in Ref.14.

Ag precipitates were examined with Zeiss 1540 XB field emission scanning electron microscopy (FESEM), JEM-ARM200CF TEM/STEM, and EBSD. The samples for FESEM and EBSD had been subjected to electropolishing in a solution of 30% H_3PO_4 and 70% deionized water with a voltage of 8 V and a current of 4 A. EBSD was performed at 20 kV, a tilt angle of

Accepted Manuscript

70°, and a scan step of 1 μm. The samples for TEM/STEM were subjected to argon ion-milling at 5 keV at 7º.

3. Results

Small discrete Ag precipitates (diameter of 7.8±1.4 nm) were found at grain boundaries in Cu-6 wt%Ag samples aged at 450 °C for 15 min (Figs. 1a, 1d). Each of these precipitates was shaped like a large, abutted cone that shared a semi-coherent interface with the Cu grain on one side of the boundary. The cone was topped by a small spherical cap that shared an uncertain type of interface with the Cu grain on the opposite side of the boundary (Figs. 1b, 1c, 1f). Because of resistance from the Zener pinning of the Ag precipitates, some grain boundaries had migrated into the form of a pronounced arc (Figs. 2a, 2b).

DPs areas were large when the Cu-6 wt%Ag sample was aged at 450 °C for 30 min (Fig. 2c). These areas, which were also observed in Cu-6 wt%Ag-0.05 wt%Sc samples, seem to have been formed between the original boundaries and reaction front, a phenomenon that has also been observed in Nickel-Base Superalloys [32]. EBSD results confirmed that the DPs in these areas had the same crystallographic orientation as the grain behind the reaction front but had a different crystallographic orientation from the grain in front of the reaction front (Fig. 3). The Ag content in the Cu matrix on both sides of the reaction front was considerably different (Fig. 4). In the DP areas, it was only 0.67±0.49 wt%, while in the non-DP areas, it was as high as 6.1± 2.1 wt%. At the migrating reaction fronts, there were some dark-contrast areas with high Ag content (Fig. 5). We suspected that they were the Ag embryos of DPs. The size of the embryos was so small, no misfit dislocation was required so that Cu/Ag interfaces were fully coherent. Apparently, large lattice distortion occurred in the vicinity of the interfaces. Once the Ag

Accepted Manuscript

embryos had grown into DPs, we found semi-coherent interfaces (Figs. 5, 6). In some regions, no lattice distortion was required to accommodate the DP formation (Fig 6).

We investigated the orientation relationship between Cu and Ag and coherency of the interfaces in order to deduce growth orientation and mechanisms of DPs using Cu-6 wt%Ag samples aged at 450 °C for 30 min and 2 h (Figs. 7, 8). The DPs close to the grain boundaries had undefined, irrational growth directions, indicating that the growth was controlled by diffusion (Figs. 8a, 8b). Away from grain boundaries, some DPs grew along [220] direction, with a coherent interface at the front and semi-coherent interfaces on the long sides (imaged at [-112] zone axis, Figs. 7, 8c), where others far from the grain boundaries grew along [3-11] (Figs. 8a, 8b). In twined area of Cu matrix, DPs grew in multiple directions. (Fig. 8d).

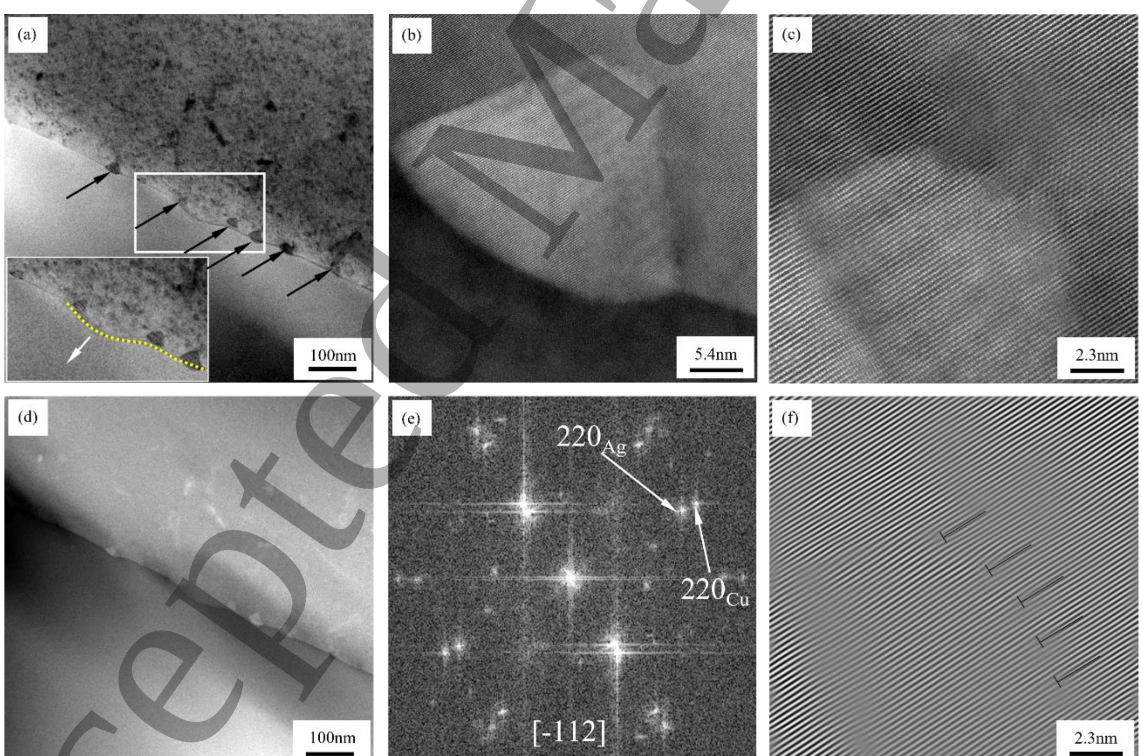

Fig. 1 STEM images showing the nucleation of Ag precipitates on grain boundaries in Cu-6 wt%Ag aged at 450 °C for 15 min. (a, d) Bright-filed STEM and high-angle annular dark-field STEM (HAADF-STEM) images of Ag precipitates. Black arrows indicate the Ag precipitates.

Accepted Manuscript

Inset shows the Ag precipitates and grain boundary at high magnification within a rectangular outline, and the white arrow indicates the direction of the grain boundary migration. (b) HAADF-STEM image of Ag precipitate at high magnification. (c) HAADF-STEM image of the Cu/Ag interface in Fig. b. (e) The corresponding Fast Fourier Transform (FFT) image of Fig. c, showing the zone axis is [-112], and the Ag precipitate tends to grow along [110] direction. (f) The corresponding Inverse Fast Fourier Transform (IFFT) image of Fig. c. “T” marks indicate the positions of misfit dislocations. From the average dislocation distance, the estimated misfit is around 10.5%. This is smaller than the misfit of bulk materials of Cu and Ag (12.1% [9]), which indicates that the misfit strain is not released completely by the misfit dislocations.

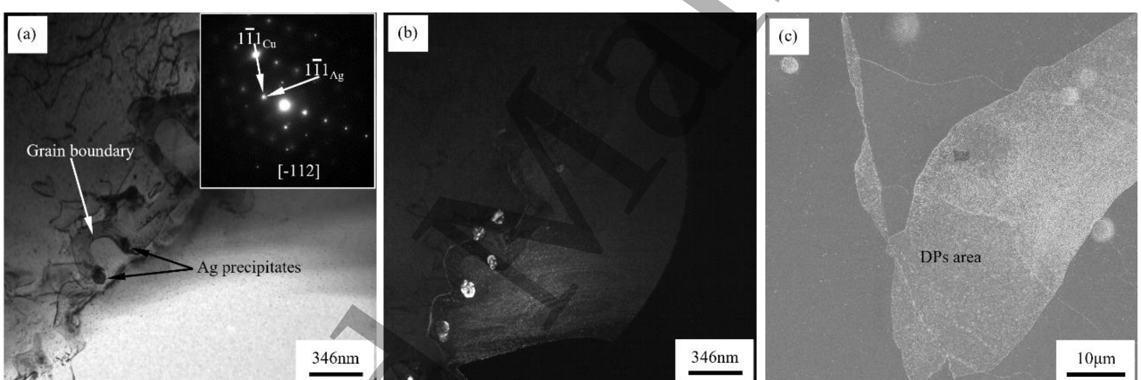

Fig. 2 TEM/SEM images showing DPs areas in samples aged at 450 °C for different times. (a, b) Bright-field and dark-field TEM images of Ag precipitates in Cu-6 wt%Ag aged for 15 min. Inset is the selected area diffraction pattern (SADP), showing the zone axis is [-112]. (c) SEM images of the DPs areas in Cu-6 wt%Ag aged for 30 min.

Accepted Manuscript

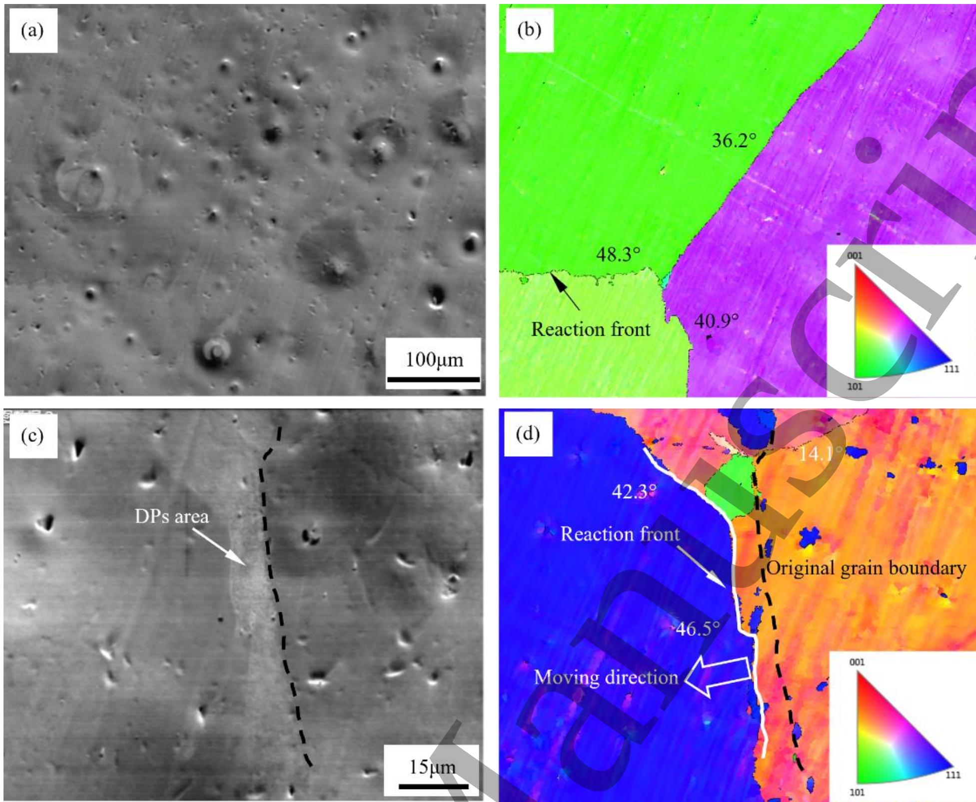

Fig. 3 SEM/EBSD images showing the crystallographic orientation of DPs areas and the grains near the reaction front in Cu-6 wt%Ag-0.05 wt%Sc aged at 450 °C for 30 min. (a, c) SEM images of DPs areas. (b, d) Corresponding EBSD images of Figs. a and c.

Accepted Manuscript

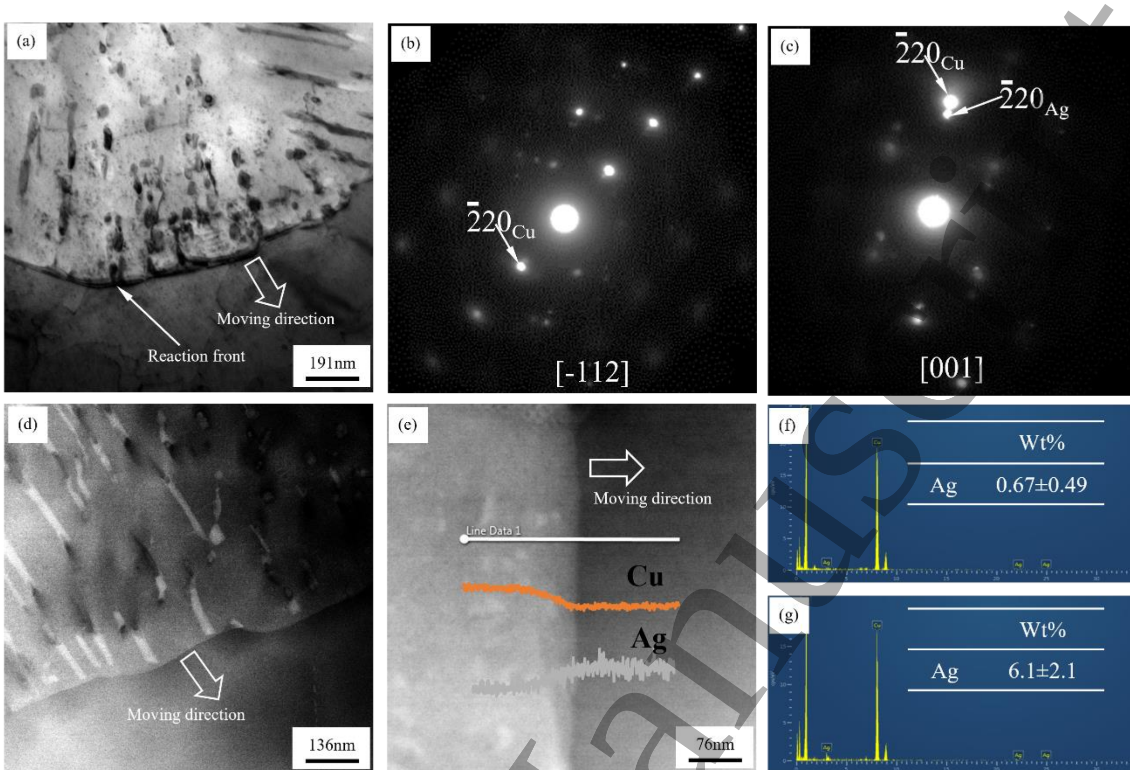

Fig. 4 TEM/STEM images showing the microstructure and element content before and after a reaction front in Cu-6 wt%Ag aged at 450 °C for 30 min. (a) Bright-field TEM image of the reaction front. (b, c) The SADP images of the areas before and after the reaction front, showing the zone axis is close to [-112] and [001], respectively. (d) HAADF-STEM image of DPs. (e) HAADF-STEM image with Ag and Cu composition profile across the reaction front. (f, g) EDS spectrum in areas before and after the reaction front, respectively.

Accepted Manuscript

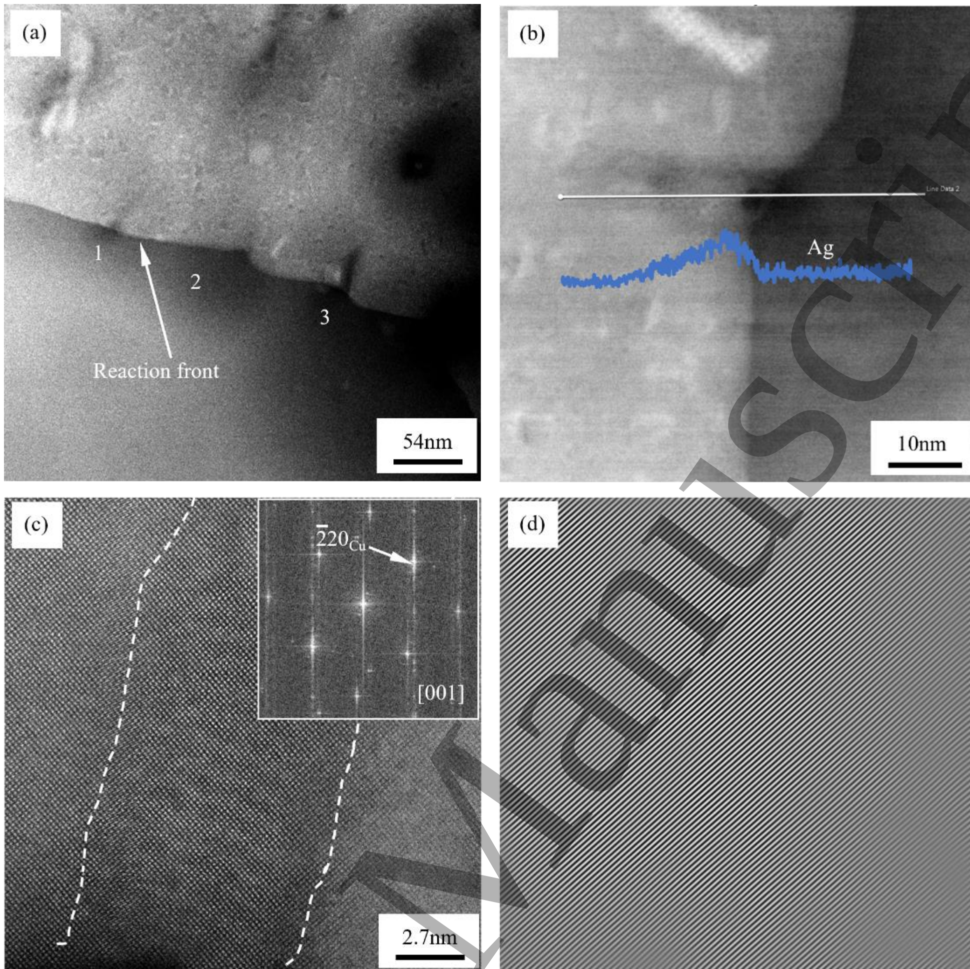

Fig. 5 HAADF-STEM images showing the embryos of DPs at a reaction front in Cu-6 wt%Ag aged at 450 °C for 30 min. (a) Embryos at the reaction front, which were marked by 1, 2, and 3. (b) The change of Ag content around embryo 2 in Fig. a. (c) High magnification of embryo 2 in Fig. a. Inset is the FFT image, showing the zone axis is [001]. (d) IFFT image of Fig. c showing a coherent Cu/Ag interface.

Accepted Manuscript

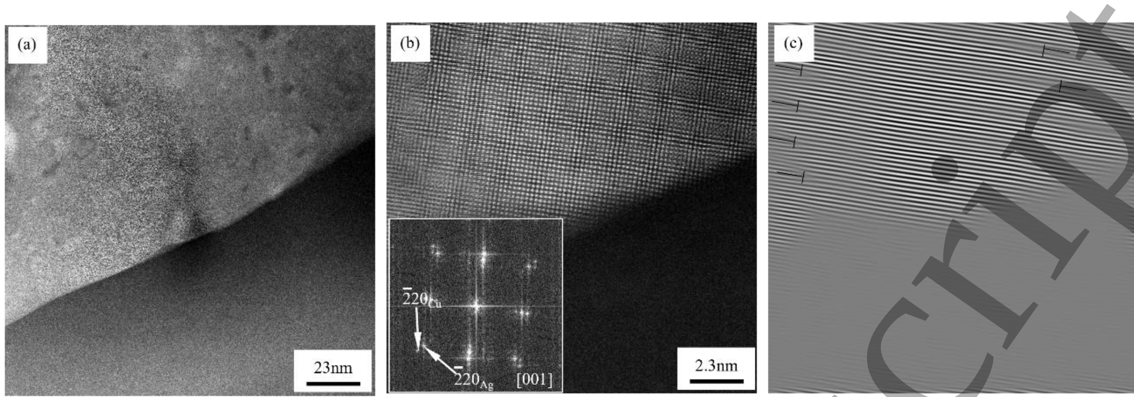

Fig. 6 HAADF-STEM images showing a discontinuous precipitate on a reaction front at Cu-6 wt%Ag aged at 450 °C for 30 min. (a) The discontinuous precipitate at the reaction front. (b) High magnification of the precipitate in Fig. a. Inset is the FFT image, showing the zone axis is [001]. (c) IFFT image of the precipitate in Fig. a, showing a semi-coherent interface. "T" marks indicate the positions of misfit dislocations. From the average dislocation distance, the estimated misfit is around 12.5%, which indicates that the misfit strain is released completely by the misfit dislocations.

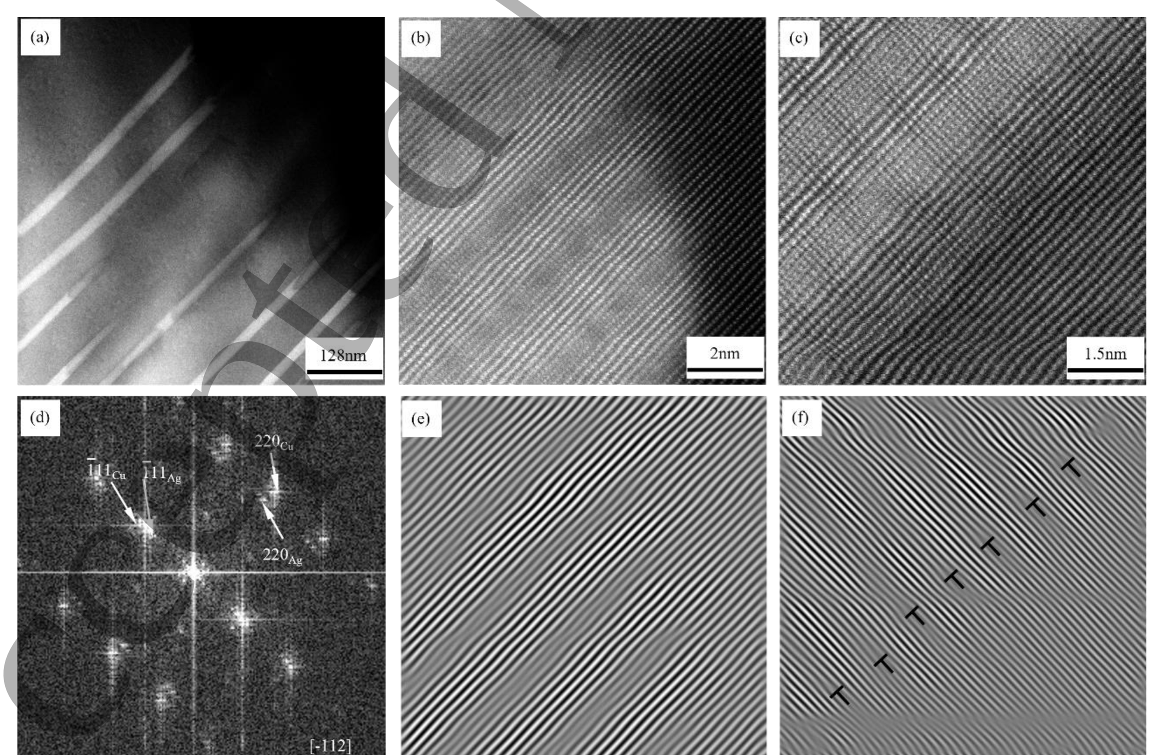

Accepted Manuscript

Fig. 7 HAADF-STEM images showing DPs at Cu-6 wt%Ag aged at 450 °C for 30 min. (a) Low magnification of DPs. (b) High magnification of the Cu/Ag interface at front of a discontinuous precipitate. (c) High magnification of the Cu/Ag interface along with a discontinuous precipitate. (d) FFT image of Fig. b, showing the zone axis is [-112]. (e) IFFT of Fig. b, showing a coherent Cu/Ag interface. (f) IFFT of Fig. c, showing a semi-coherent Cu/Ag interface. "T" marks indicate the positions of misfit dislocations. From the average dislocation distance, the estimated misfit is around 9.9%, which indicates that the misfit strain is not released completely by the misfit dislocations.

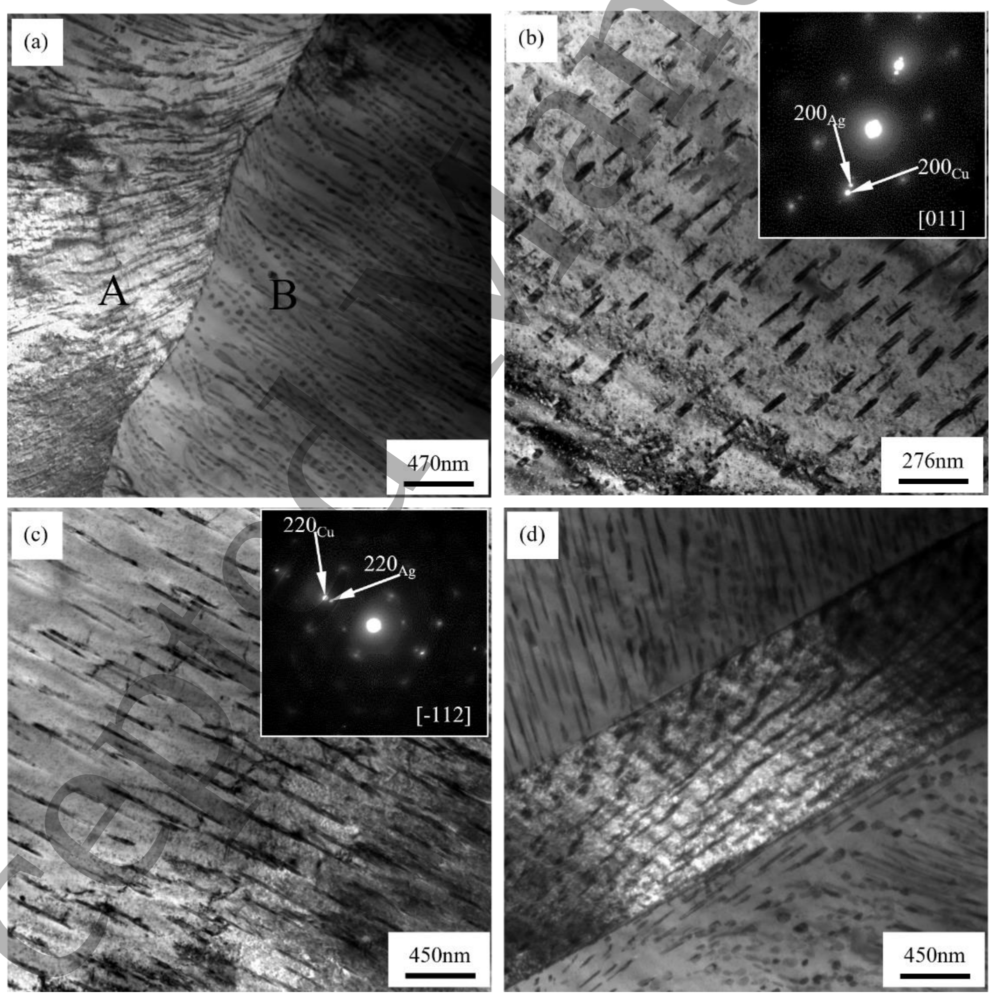

Fig. 8 TEM images showing DPs in Cu-6 wt%Ag aged at 450 °C for 2 h. (a) DPs near a grain boundary. (b) DPs far away from the grain boundary in grain A. Inset in Fig. b is the SADP

Accepted Manuscript

image of A grain, showing the zone axis is [011]. (c) DPs far away from a grain boundary. Inset is the SADP image of Fig. c, showing the zone axis is [-112]. (d) DPs, which grow in multiple directions, near twin boundaries.

4. Discussion

In our current work, we found that lattice distortion always occurred in the presence of DPs, whether or not the alloy had been previously doped with Sc. This distortion resulted in both shape anisotropy and internal stress anisotropy [33, 34]. Sc was added to partially suppress DPs in order to understand if our finding can be applied to broader systems.

We observed individual formation of nuclei at the grain boundaries similar to that proposed by Tu and Turnbull et al. [20, 21]. All the nuclei in our alloys were Ag particles that had nucleated heterogeneously at Cu grain boundaries. This is similar to what happens in most heterogeneous nucleation, such as Widmannstätten ferrite nucleation in steels [35, 36]. Each shape-anisotropic nucleus had a spherical cap on one side and a cone on the other (Fig. 9). According to heterogeneous nucleation theory, incoherent interfaces usually optimize their shape into spherical caps [37]. Thus, we assumed that the cap-shaped part had an incoherent Cu/Ag interface with a Cu grain on the opposite side of the boundary. Our STEM images showed that each cone-shaped part, on the other hand, had a semi-coherent Cu/Ag interface with a Cu grain on the opposite side of the boundary. Growth on the cone side of a Ag nucleus along a semi-coherent Cu/Ag interface would necessarily be very slow because of the ledge mechanism. Growth on the cap-shaped side, however, would be faster because incoherent interfaces could be expected to have higher mobility and higher energy in the early stages of nucleation. The difference in speed of growth between the two sides meant that the Cu/Ag interfaces moved mainly in one direction. This unidirectional migration caused the growth of Ag in the same

Accepted Manuscript

direction. The exhaustion of Ag from nearby Cu brought about Cu grain-boundary migration in the same direction, otherwise known as cooperative growth of Cu and Ag, which indicates that discontinuous precipitation has occurred.

We observed the curved grain boundary that indicated that migration has occurred. Its energy change (ΔG_g) can be expressed as follows [38]:

$$\Delta G_g = \frac{\gamma_{Cu/Cu'} V_m}{r} \quad (1)$$

where $\gamma_{Cu/Cu'}$ is the grain boundary energy in Cu-Ag alloy, V_m is the molar volume, r is the radius of the grain boundary. At the beginning of grain boundary migration in solution-treated Cu-Ag samples, 2r was as large as the average grain size, which caused a very small G_g. When the migrating grain boundaries were pinned by Ag nuclei, 2r decreased rapidly, thus increasing G_g and helping the boundaries grow along with the Ag (Figs. 2a, 2c). DPs nucleate easily at high-angle grain boundaries because these boundaries typically have high $\gamma_{Cu/Cu'}$ [27]. We speculate that small-sized grains and high grain boundary energy will promote grain boundary migration, thus triggering discontinuous precipitation.

Once the Cu grains and the Ag nuclei had established a cooperative growth mode, DPs began to grow via migrating boundaries (Fig. 4). If one of the phases had had bcc structure, as previous researchers observed in Cu/Nb, the Kurdjumov-Sachs or Nishiyama–Wasserman relationship might have occurred [39-41]. At this stage in our study, however, FCC Cu and Ag established a cube-on-cube orientation relationship. The cooperative growth consumed supersaturated solid solution and caused energy change (ΔG), which can be expressed as follows [38]:

$$\Delta G = a\Delta G_0 + b\gamma_{Cu/Ag} V_m + \frac{\gamma_{Cu/Cu'} V_m}{r} \quad (2)$$

Accepted Manuscript

where $a\Delta G_0$ is the energy released during discontinuous precipitation, in which a is the fraction of total energy (ΔG_0), $b\gamma_{Cu/Ag}$ is the part of the energy that converts to the Cu/Ag interface energy, in which b is associated with the size and shape of Ag precipitates. We calculated ΔG_0 using follow equation [22, 42]:

$$\Delta G_0 = \mathrm{R}T[X_{\alpha}^{'}\ln\frac{X_{\alpha e}}{X_{\alpha}^{'}} + (1 - X_{\alpha}^{'})\ln\frac{(1 - X_{\alpha e})}{(1 - X_{\alpha}^{'})}] \quad (3)$$

where R is the gas constant (8.314 J/K/mol), T is the aging temperature (450 °C in our study), $X_{\alpha}^{'}$ is the fraction of Ag in supersaturated Cu (3.68 atom%, from our EDS results, see Fig. 4g), $X_{\alpha e}$ is the equilibrium solubility of Ag in Cu at 450 °C (0.35 atom%, according to phase diagram [43]). Our calculation showed that the released energy, ΔG_0, was -323.7 J/mol. In Eq. 2, b is $2/S$ [44], in which S is the spacing of DPs (77.8±35.6 nm, see Figs. 4a, 4d). $\gamma_{Cu/Ag}$ is the energy of the coherent Cu/Ag interface (estimated as 0.23 J/mol by Bacher et al and Bouvalet et al. [45, 46]). r is the radius of migrating grain boundaries (about 838 nm, see Fig. 4a). Taking a as 0.5, our calculation showed that ΔG was -112.9 J/mol, where -161.8 J/mol came from the difference between the Ag solute in different phases, 43.2 J/mol came from the Cu/Ag interfaces, and 5.7 J/mol came from the curved boundaries. This means that when discontinuous precipitation is steadily proceeding, the greater the solute difference between the two sides of the grain, the higher the driving energy for grain boundary migration.

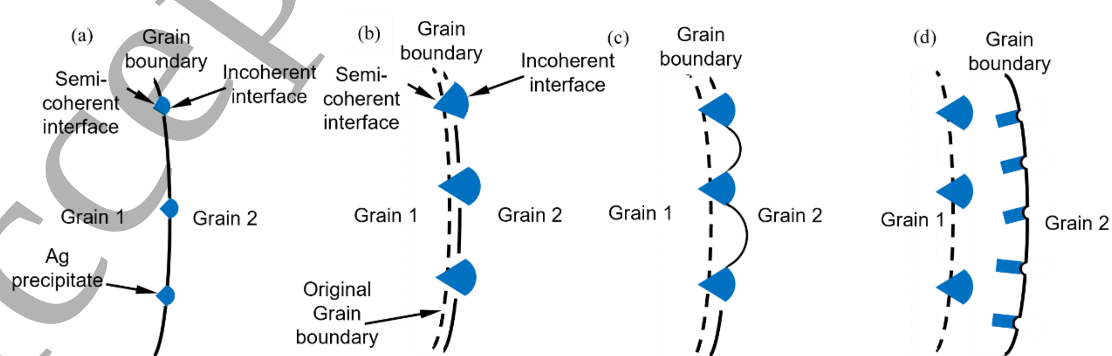

Accepted Manuscript

Fig. 9 Schematic illustrations of nucleation and growth of DPs in Cu-Ag alloys.

5. Conclusion

1. When Ag was a solute in Cu-Ag alloys, the nuclei of discontinuous precipitation was always Ag phase, which formed as multiple precipitates at grain boundaries, taking a unique shape of abutted large-sized cone (semi-coherent interface) and small-sized spherical cap (incoherent interface). This unique shape near the interfaces caused the difference of interface energy in two kinds of interfaces, leading to interface growth in one type of interface. The growth of the Ag precipitates drained Ag from surrounding Cu so that new Cu grain migrated with Ag to form discontinuous precipitates.

2. The misfit value between Cu and Ag in DPs was below that of the bulk materials in some cases. At some interfaces, the misfit was zero. This indicated that lattice distortion occurred DPs. The lattice distortion, which was related to the dimension of the interfaces, led to anisotropy in shape, orientation, and stress in the materials. The excessive energy of this lattice distortion provided part of the driving force for formation of DPs.

3. DPs formed between the original boundaries and reaction front. The Ag solute difference on both sides of the reaction front was as large as about 5.4 wt%, which produced driving force for grain boundary migration.

Acknowledgements

This work was supported by the National Key R&D Program of China [Grant No. 2017YFE0107900] and the 111 Project (2.0) of China [Grant No. BP0719037]. Additional financial support was provided by the China Scholarship Council. Some work was performed at the National High Magnetic Field Laboratory (NHMFL), USA, which is supported by National Science Foundation Cooperative Agreement [Grant No. DMR-1157490 and NSF DMR-1644779]

Accepted Manuscript

and the State of Florida, USA. The authors are grateful to Robert E. Goddard and YiFeng Su from NHMFL for SEM and TEM training.

Declaration of competing interest

The authors declare that they have no competing, personal and financial interests in this manuscript.

Data availability statement

All data that support the findings of this study are included within the article (and any supplementary files).

Reference

[1] K. Han, J.D. Embury, J.R. Sims, L.J. Campbell, H.J. Schneider-Muntau, V.I. Pantsyrnyi, A. Shikov, A. Nikulin, A. Vorobieva, The fabrication, properties and microstructure of Cu-Ag and Cu-Nb composite conductors, Mater. Sci. Eng. A 267(1) (1999) 99-114.
[2] K. Han, A. Baca, H. Coe, J. Embury, K. Kihara, B. Lesch, L. Li, J. Schillig, J. Sims, S.V. Sciver, H.J. Schneider-Muntau, Material issues in the 100 T non-destructive magnet, IEEE Trans. Appl. Supercond. 10(1) (2000) 1277-1280.
[3] Y. Sakai, K. Inoue, H. Maeda, New high-strength, high-conductivity Cu-Ag alloy sheets, Acta Metall. 43(4) (1995) 1517-1522.
[4] K. Han, R. Niu, J. Lu, V. Toplosky, High strength conductors and structural materials for high field magnets, RSC Adv. 1(17) (2016) 1233-1239.
[5] K. Han, R. Walsh, V. Toplosky, J. Lu, High strength conductors for high field magnets, TMS annual meeting supplemental proceedings: materials properties, characterization, and modeling, John Wiley & Sons, Inc., 2012, pp. 521-528.
[6] X. Zuo, K. Han, C. Zhao, R. Niu, E. Wang, Microstructure and properties of nanostructured Cu28wt%Ag microcomposite deformed after solidifying under a high magnetic field, Mater. Sci. Eng. A 619 (2014) 319-327.
[7] A. Gaganov, J. Freudenberger, W. Grünberger, L. Schultz, Microstructural evolution and its effect on the mechanical properties of Cu–Ag microcomposites, Z. MetaIlkd. 95(6) (2004) 425-432.
[8] K. Han, J. Lu, V. Toplosky, R. Niu, R. Goddard, Y. Xin, R. Walsh, I. Dixon, V. Pantsyrny, Properties of selected high-strength composite conductors with different strengthening components, IEEE Trans. Appl. Supercond. 30(4) (2020) 1-5.
[9] J.B. Liu, L. Zhang, D.W. Yao, L. Meng, Microstructure evolution of Cu/Ag interface in the Cu-6 wt.% Ag filamentary nanocomposite, Acta Mater. 59(3) (2011) 1191-1197.
[10] C. Zhao, X. Zuo, E. Wang, R. Niu, K. Han, Simultaneously increasing strength and electrical conductivity in nanostructured Cu-Ag composite, Mater. Sci. Eng. A 652 (2016) 296-304.

Accepted Manuscript

[11] K. Han, G.D.W. Smith, D.V. Edmonds, Pearlite phase transformation in Si and V steel, Metall. Mater. Trans. A 26(7) (1995) 1617-1631.
[12] K.N. Braszczyńska-Malik, Discontinuous and continuous precipitation in magnesium–aluminium type alloys, J. Alloys Compd. 477(1) (2009) 870-876.
[13] S. Ueta, M. Hida, M. Kajihara, Effects of Fe, W and Mo on kinetics of discontinuous precipitation in the Ni-Cr system, Mater. Trans. 53(10) (2012) 1744-1752.
[14] B. An, Y. Xin, R. Niu, J. Lu, E. Wang, K. Han, Hardening Cu-Ag composite by doping with Sc, Mater. Lett. 252 (2019) 207-210.
[15] J.B. Liu, L. Meng, Phase orientation, interface structure, and properties of aged Cu-6 wt.% Ag, J. Mater. Sci. 43(6) (2008) 2006-2011.
[16] T. Rojhirunsakool, S. Nag, R. Banerjee, Discontinuous precipitation of γ' phase in Ni-Co-Al alloys, JOM 66(8) (2014) 1465-1470.
[17] S. Semboshi, J. Ikeda, A. Iwase, T. Takasugi, S. Suzuki, Effect of boron doping on cellular discontinuous precipitation for age-hardenable Cu-Ti alloys, Materials 8(6) (2015) 3467-3478.
[18] I. Manna, S.K. Pabi, W. Gust, Discontinuous reactions in solids, Int. Mater. Rev. 46(2) (2001) 53-91.
[19] I. Manna, Grain boundary migration in solid state discontinuous reactions, Interface Sci. 6(1) (1998) 113-131.
[20] K.N. Tu, D. Turnbull, Morphology of cellular precipitation of tin from lead-tin bicrystals, Acta Metall. 15(2) (1967) 369-376.
[21] K.N. Tu, D. Turnbull, Morphology of cellular precipitation of tin from lead-tin bicrystals-ii, Acta Metall. 15(8) (1967) 1317-1323.
[22] R.A. Fournelle, J.B. Clark, The genesis of the cellular precipitation reaction, Metall. Mater. Trans. B 3(11) (1972) 2757-2767.
[23] P. Zieba, Recent developments on discontinuous precipitation, Arch. Metall. Mater. 62(2) (2017) 955-968.
[24] S. Semboshi, M. Sato, Y. Kaneno, A. Iwase, T. Takasugi, Grain boundary character dependence on nucleation of discontinuous precipitates in Cu-Ti alloys, Materials 10(4) (2017) 415.
[25] M. Tałach-Dumańska, P. Zięba, A. Pawłowski, J. Wojewoda, W. Gust, Practical aspects of discontinuous precipitation and dissolution, Mater. Chem. Phys. 80(2) (2003) 476-481.
[26] R. Monzen, H. Shigehara, K. Kita, Misorientation dependence of discontinuous precipitation in Cu-Be alloy bicrystals, J. Mater. Sci. 35(23) (2000) 5839-5843.
[27] R. Monzen, C. Watanabe, D. Mino, S. Saida, Initiation and growth of the discontinuous precipitation reaction at [011] symmetric tilt boundaries in Cu–Be alloy bicrystals, Acta Mater. 53(4) (2005) 1253-1261.
[28] S.P. Gupta, Kinetics of discontinuous precipitation and dissolution in Cu–Ag alloys, Can. Metall. Q. 37(2) (1998) 141-159.
[29] I. Manna, S.K. Pabi, A study of the nucleation characteristics of discontinuous precipitation in a pro-eutectic Cu-Ag alloy, J. Mater. Sci. Lett. 9(10) (1990) 1226-1228.
[30] D. Hamana, M. Hachouf, L. Boumaza, Z.E.A. Biskri, Precipitation kinetics and mechanism in Cu-7 wt% Ag alloy, Mater. Sci. Appl 2(7) (2011) 899-910.
[31] R. Monzen, T. Terazawa, C. Watanabe, Effect of an applied stress on discontinuous precipitation in a Cu-Ag alloy, in: W. Skrotzki, C.G. Oertel, H. Biermann, M. Heilmaier (Eds.), 15th International Conference on the Strength of Materials, 2010.

Accepted Manuscript

[32] A. Heckl, S. Cenanovic, M. Göken, R.F. Singer, Discontinuous precipitation and phase stability in Re- and Ru-containing Nickel-base superalloys, Metall. Mater. Trans. A 43(1) (2012) 10-19.
[33] K. Han, A. Lawson, J. Wood, J. Embury, R. Von Dreele, J. Richardson, Internal stresses in cold-deformed Cu–Ag and Cu–Nb wires, Philos. Mag. 84(24) (2004) 2579-2593.
[34] T. Shen, X. Zhang, K. Han, C. Davy, D. Aujla, P. Kalu, R. Schwarz, Structure and properties of bulk nanostructured alloys synthesized by flux-melting, J. Mater. Sci. 42(5) (2007) 1638-1648.
[35] H. Li, L. Wang, H. Xiao, J. Xu, S. Zheng, Q. Zhai, K. Han, Hardening Low-Carbon Steels by Engineering the Size and Distribution of Inclusions, Metallurgical and Materials Transactions A 50(1) (2019) 336-347.
[36] H. Xiao, S. Zheng, Y. Xin, J. Xu, K. Han, H. Li, Q. Zhai, Characterization of Microstructure in High-Hardness Surface Layer of Low-Carbon Steel, 10(8) (2020) 995.
[37] D.A. Porter, K.E. Easterling, Phase transformations in metals and alloys, Second ed., CRC Press, New York, 1992. 271-287.
[38] R.D. Knutsen, C.I. Lang, J.A. Basson, Discontinuous cellular precipitation in a Cr–Mn–N steel with niobium and vanadium additions, Acta Mater. 52(8) (2004) 2407-2417.
[39] K. Yu-Zhang, J.D. Embury, K. Han, A. Misra, Transmission electron microscopy investigation of the atomic structure of interfaces in nanoscale Cu–Nb multilayers, Philos. Mag. 88(17) (2008) 2559-2567.
[40] L. Deng, X. Yang, K. Han, Y. Lu, M. Liang, Q. Liu, Microstructure and texture evolution of Cu–Nb composite wires, Mater. Charact. 81 (2013) 124-133.
[41] A. Ishmaku, K.P. Han, Characterization of Cold-Rolled Cu-Nb Composite, Mater. Sci. Forum 453-454 (2004) 479-484.
[42] J.M. Shapiro, The kinetics of discontinuous precipitation in copper indium alloys, [D]. Hamilton, McMaster University, 1966.
[43] R.P. Elliott, F.A. Shunk, W.C. Giessen, The Ag−Cu (silver-copper) system, Bull. Alloy Phase Diagr. 1(1) (1980) 41.
[44] J.W. Cahn, The kinetics of cellular segregation reactions, Acta Metall. 7(1) (1959) 18-28.
[45] P. Bacher, P. Wynblatt, S.M. Foiles, A Monte Carlo study of the structure and composition of (001) semicoherent interphase boundaries in Cu-Ag-Au alloys, Acta Metall. 39(11) (1991) 2681-2691.
[46] M. Bonvalet, X. Sauvage, D. Blavette, Intragranular nucleation of tetrahedral precipitates and discontinuous precipitation in Cu-5wt%Ag, Acta Mater. 164 (2019) 454-463.

Accepted Manuscript